DIACYLGLYCEROL ACYLTRANSFERASE and DIACYLGLYCEROL KINASE Modulate Triacylglycerol and Phosphatidic Acid Production in the Plant Response to Freezing Stress[1]

Wei-Juan Tan, Yi-Cong Yang, Ying Zhou, Li-Ping Huang, Le Xu, Qin-Fang Chen, Lu-Jun Yu,[2] and Shi Xiao[2]

State Key Laboratory of Biocontrol, Guangdong Provincial Key Laboratory of Plant Resources, School of Life Sciences, Sun Yat-sen University, Guangzhou 510275, China

ORCID ID: 0000-0002-6632-8952 (S.X.)

Plants accumulate the lipids phosphatidic acid (PA), diacylglycerol (DAG), and triacylglycerol (TAG) during cold stress, but how plants balance the levels of these lipids to mediate cold responses remains unknown. The enzymes ACYL-COENZYME A:DIACYLGLYCEROL ACYLTRANSFERASE (DGAT) and DIACYLGLYCEROL KINASE (DGK) catalyze the conversion of DAG to TAG and PA, respectively. Here, we show that DGAT1, DGK2, DGK3, and DGK5 contribute to the response to cold in Arabidopsis (*Arabidopsis thaliana*). With or without cold acclimation, the *dgat1* mutants exhibited higher sensitivity upon freezing exposure compared with the wild type. Under cold conditions, the *dgat1* mutants showed reduced expression of *C-REPEAT/DRE BINDING FACTOR2* and its regulons, which are essential for the acquisition of cold tolerance. Lipid profiling revealed that freezing significantly increased the levels of PA and DAG while decreasing TAG in the rosettes of *dgat1* mutant plants. During freezing stress, the accumulation of PA in *dgat1* plants stimulated NADPH oxidase activity and enhanced RbohD-dependent hydrogen peroxide production compared with the wild type. Moreover, the cold-inducible transcripts of *DGK2*, *DGK3*, and *DGK5* were significantly more up-regulated in the *dgat1* mutants than in the wild type during cold stress. Consistent with this observation, *dgk2*, *dgk3*, and *dgk5* knockout mutants showed improved tolerance and attenuated PA production in response to freezing temperatures. Our findings demonstrate that the conversion of DAG to TAG by *DGAT1* is critical for plant freezing tolerance, acting by balancing TAG and PA production in Arabidopsis.

Cold stresses, including chilling and freezing, are major environmental factors that severely restrict plant growth, development, productivity, and ecological distribution. Most temperate plants have evolved complex strategies, such as transcriptome reprogramming and biochemical membrane remodeling, to survive low temperatures (Thomashow, 1999). The INDUCER OF CBF EXPRESSION (ICE)-C-REPEAT BINDING FACTOR/DRE BINDING FACTOR1 (CBF/DREB1) transcriptional cascade is a well-established cold signaling pathway in Arabidopsis (*Arabidopsis thaliana*; Thomashow, 1999; Chinnusamy et al., 2007). The basic helix-loop-helix transcription factor ICE1 directly targets cis-elements in the *CBF3/DREB1a* and *CBF2* promoters (Chinnusamy et al., 2007). In contrast, ICE2 (the paralog of ICE1) is associated with the transcriptional regulation of *CBF1/DREB1b* (Fursova et al., 2009).

Besides the core ICE-CBF/DREB1 module, plant cells undergo significant alterations of both plastidic and extraplastidic membrane lipids in response to cold temperatures, thus preventing membrane injury and cellular dehydration (Uemura et al., 1995; Welti et al., 2002; Moellering et al., 2010). Under chilling and freezing conditions, unsaturated fatty acid and phospholipid (PL) levels increase rapidly to maintain the fluidity and integrity of membrane structure, thereby enhancing plant tolerance to such stresses (Kuiper, 1970; Welti et al., 2002). In Arabidopsis, two phospholipase Ds (PLDs), PLDα1 and PLDδ, are involved in the cold-induced hydrolysis of membrane PLs to produce phosphatidic acid (PA; Welti et al., 2002; Li et al., 2004; Rajashekar et al., 2006). The *PLDα1* knockout mutants have reduced cold-responsive accumulation of PA and enhanced freezing tolerance (Welti et al., 2002; Rajashekar et al., 2006), but the *PLDδ* knockout mutants have decreased freezing tolerance (Li et al., 2004). The opposite freezing sensitivities observed between the *PLDα1* and *PLDδ* knockout mutants are likely caused by PLDα1-triggered reactive oxygen species (ROS) production and PLDδ-mediated ROS

[1]This work was supported by the National Key R&D Program of China (Project 2016YFD0400103), the National Natural Science Foundation of China (Projects 31725004 and 31670276), and the Natural Science Foundation of Guangdong Province, China (Project 2017A030308008).

[2]Address correspondence to yulujun2@mail.sysu.edu.cn or xiaoshi3@mail.sysu.edu.cn.

The author responsible for distribution of materials integral to the findings presented in this article in accordance with the policy described in the Instructions for Authors (www.plantphysiol.org) is: Shi Xiao (xiaoshi3@mail.sysu.edu.cn).

S.X. designed the research; W.-J.T., Y.-C.Y., Y.Z., L.-P.H. L.X., and Q.-F.C carried out the experiments; S.X., W.-J.T., and L.-J.Y. analyzed the data; S.X., W.-J.T., and L.-J.Y. wrote the article.

www.plantphysiol.org/cgi/doi/10.1104/pp.18.00402

mitigation (Zhang et al., 2003, 2009b). Interestingly, both PLDα1- and PLDδ-mediated plant cold sensitivities are independent of the CBF/DREB pathway (Welti et al., 2002; Li et al., 2004; Rajashekar et al., 2006), which indicates an alternative mechanism in regulating cold tolerance in plants. Previous findings further reveal that a deficiency of *SENSITIVE TO FREEZING2* (*SFR2*), a gene encoding a galactolipid-remodeling enzyme located in the chloroplast outer envelope membrane, confers an extremely freezing-sensitive phenotype (Thorlby et al., 2004; Fourrier et al., 2008; Moellering et al., 2010). Under freezing conditions, SFR2 transfers the galactosyl residues from monogalactosyldiacylglycerol (MGDG) to different galactolipid acceptors to produce oligogalactolipids and diacylglycerol (DAG).

Increasing evidence suggests that the polar lipid PA, which lacks a head group, can form a destabilized hexagonal II (H_{II})-type phase with MGDG or DAG (Steponkus, 1984; Uemura et al., 1995; Thomashow, 1999; Welti et al., 2002; Moellering et al., 2010; Moellering and Benning, 2011), damaging the cell membrane during freezing-induced dehydration. Conversely, the removal of these lipids may prevent H_{II} membrane formation and improve recovery from cold stress.

DAG is likely converted to triacylglycerol (TAG) by the enzyme ACYL-COENZYME A:DIACYLGLYCEROL ACYLTRANSFERASE (DGAT), which may play an important role in the removal of excess DAG after freezing (Moellering et al., 2010; Moellering and Benning, 2011). Moreover, recent studies suggest that, in response to cold stresses, DAG can be phosphorylated by DIACYLGLYCEROL KINASE (DGK) to produce PA (Gómez-Merino et al., 2004; Arisz et al., 2013). Our recent work indicates that the disruption of three genes encoding lipase-like proteins, *SENESCENCE-ASSOCIATED GENE101* (*SAG101*), *ENHANCED DISEASE SUSCEPTIBILITY1* (*EDS1*), and *PHYTOALEXIN DEFICIENT4* (*PAD4*), confers salicylic acid (SA)-mediated freezing tolerance (Chen et al., 2015b). The mutants showed significantly lower levels of DAG and PA and higher levels of TAG than the wild type, suggesting that SA is likely involved in the regulation of cold-responsive lipid remodeling in plants. Consistent with this, the application of SA suppresses the cold-induced expression of *DGATs* and *DGKs* in wild-type leaves (Chen et al., 2015b). It is conceivable, therefore, that DAG may act as a common substrate for PA and TAG production upon cold exposure, the homeostasis of which may determine plant tolerance to such stresses. However, it is still unknown how the enzymes downstream of DAG contribute to the balance of TAG and PA production under freezing conditions.

The Arabidopsis genome has three *DGAT* genes (*DGAT1–DGAT3*) and seven *DGK* genes (*DGK1–DGK7*). DGAT1 is involved in TAG biosynthesis and lipid deposition in Arabidopsis seeds (Routaboul et al., 1999; Saha et al., 2006; Shockey et al., 2006; Hernández et al., 2012). However, the precise cellular functions of Arabidopsis DGKs remain elusive. In this study, we show that the *dgat1* null mutants (*dgat1-1* and *dgat1-2*) were more sensitive to chilling and freezing stresses compared with the wild type. Upon freezing exposure, lipid profile analysis revealed that TAG decreased significantly and DAG and PA accumulated more in the *dgat1* mutants in comparison with the wild type. In addition, we observed that the knockout mutants of *DGK2*, *DGK3*, and *DGK5* conferred enhanced tolerance to freezing stress. These results, together with the finding that freezing-induced PA accumulation declines significantly in the *dgk* mutants, suggest that the modulation of DAG conversion to TAG and PA by DGATs and DGKs, respectively, plays an important role in plant responses to cold stress.

RESULTS

DGAT1 Expression Is Cold Inducible

To evaluate the potential involvement of DGAT1 in the response to cold, 4-week-old wild-type (ecotype Columbia-0) plants were subjected to chilling (4°C) conditions, and the temporal pattern of *DGAT1* expression was determined using reverse transcription quantitative PCR (RT-qPCR). The transcript of *PHOSPHOLIPID:DIACYLGLYCEROL ACYLTRANSFERASE1* (*PDAT1*), another DAG acyltransferase in Arabidopsis, also was tested as a control. The results showed that *DGAT1* expression was up-regulated from 3 to 96 h upon cold exposure, with levels increasing 197- and 43-fold in the shoots and the roots, respectively, at 96 h (Supplemental Fig. S1A). However, in the shoot tissues, cold stress (4°C) had little effect on the level of *PDAT1* transcript, which was only elevated slightly at 1, 12, 24, and 48 h following cold treatment (Supplemental Fig. S1A). Consistent with our findings, data from a publicly available microarray database (http://www.bar.utoronto.ca/efp/cgi-bin/efpWeb.cgi; Kilian et al., 2007) showed that the expression of *DGAT1*, but not *PDAT1*, was induced in response to cold stress (Supplemental Fig. S1B). Therefore, it appears that DGAT1 may play a role in the response to cold in Arabidopsis.

The *dgat1* Mutants Exhibit Reduced Tolerance to Chilling and Freezing Stresses

To investigate the function of *DGAT1* in plant responses to cold stress, two previously characterized *DGAT1* mutants, *dgat1-1* and *dgat1-2* (Routaboul et al., 1999; Xu et al., 2012), were obtained and used for phenotypic analysis (Supplemental Fig. S2). Under normal growth conditions, the 3-week-old *dgat1-1* and *dgat1-2* mutants showed no visible growth defects in comparison with the wild type (Supplemental Fig. S3A, top). However, when 3-week-old plants were exposed to 4°C for another 3 weeks, the rosettes of both *dgat1-1* and *dgat1-2* mutants became browner and yellower compared with the wild-type rosettes under the same conditions (Supplemental Fig. S3A, bottom). Trypan Blue

and 3,3′-diaminobenzidine (DAB) staining showed that more significant cell death and hydrogen peroxide (H_2O_2) accumulation occurred in the cold-treated *dgat1-1* and *dgat1-2* rosettes in comparison with the wild type (Supplemental Fig. S3, B and C).

The sensitivities of *dgat1-1* and *dgat1-2* mutant plants to freezing temperatures were tested further and compared with those of the wild-type plants. Four-week-old wild-type, *dgat1-1*, and *dgat1-2* plants that were nonacclimated (NA) or cold acclimated (CA; 4°C for 3 d) were further exposed to various freezing temperatures. When the NA plants were treated at −6°C and −8°C for 40 min followed by a 5-d recovery period in normal conditions, the *dgat1-1* and *dgat1-2* mutants were more sensitive to the freezing stress than wild-type plants (Fig. 1A). Statistical analysis of the survival rates confirmed that, after the 5-d recovery period, most of the *dgat1* mutant plants died, with survival rates of ∼45% and ∼20% at −6°C and −8°C, respectively (Fig. 1B). However, most of the wild-type plants (75%) survived at temperatures as low as −6°C, and 45% survived at −8°C (Fig. 1B). After acclimation at 4°C for 3 d, the freezing tolerance of wild-type plants increased (Fig. 1E), as indicated by the increase in survival rate from 45% in NA to 65% in CA at −8°C (Fig. 1F). Survival also increased in the *dgat1* mutants at −8°C, from 20% in the NA treatment to ∼30% in the CA treatment, but it was only ∼10% in the CA treatment at −10°C (Fig. 1, E and F). The reduced freezing tolerance of the *dgat1-1* and *dgat1-2* plants compared with the wild type was further confirmed by measuring their dry weight upon exposure to NA or CA freezing temperatures (Fig. 1, C and G).

To verify the damage to membrane integrity after freezing treatment, we analyzed electrolyte leakage in rosettes collected from the NA and CA freezing-treated wild-type, *dgat1-1*, and *dgat1-2* plants. Under NA freezing conditions, the *dgat1-1* and *dgat1-2* mutants exhibited significantly higher ionic leakage than wild-type plants at −6°C, −7°C, and −8°C (Fig. 1D). The ionic leakage rates also were elevated significantly in the CA freezing-treated *dgat1-1* and *dgat1-2* rosettes at −8°C, −9°C, and −10°C compared with wild-type plants (Fig. 1H). These findings suggest that mutation of *DGAT1* attenuates the plant tolerance to chilling and freezing stresses.

H_2O_2 and SA Accumulate in the *dgat1* Mutants upon Exposure to Freezing Temperatures

Freezing stress triggers the accumulation of ROS and cell death in plant rosette leaves (Iba, 2002; Chen et al., 2015b). To further investigate the increased sensitivity of *dgat1* mutants to freezing stresses involving ROS and cell death, we employed DAB and Trypan Blue staining assays to examine the levels of H_2O_2 and cell death in wild-type, *dgat1-1*, and *dgat1-2* mutant plants during CA, freezing, and postfreezing recovery conditions. Under 22°C or CA conditions, the wild-type and mutant leaves showed few significant signals in both staining assays (Fig. 2). In contrast, after exposure to freezing temperatures (−8°C for NA and −10°C for CA plants), elevated H_2O_2 accumulation and more severe cell death were detected in the *dgat1-1* and *dgat1-2* mutants in comparison with the wild-type leaves (Fig. 2, A and B).

The accumulation of ROS in the *dgat1* mutants in response to freezing exposure was further confirmed using an Amplex Red-coupled fluorescence quantitative assay. Consistent with the DAB staining, the H_2O_2 levels showed no significant difference between the wild type and *dgat1* mutants at 22°C and CA conditions (Fig. 2C). Under NA −8°C, CA −10°C, and postfreezing recovery conditions, H_2O_2 accumulated to a greater degree in the *dgat1-1* and *dgat1-2* mutants in comparison with the wild-type plants (Fig. 2C).

Since freezing stress induces the accumulation of SA, which contributes to freezing-induced ROS production and plant freezing sensitivity (Miura and Ohta, 2010; Kim et al., 2013; Chen et al., 2015b), we next measured the endogenous SA levels in wild-type and *dgat1* mutant rosettes under various temperature conditions. Consistent with previous findings, the freezing treatment induced SA levels in wild-type rosettes compared with the 22°C or CA conditions (Fig. 2D). In contrast, in response to both the NA −8°C and CA −10°C treatments, SA levels were much higher in *dgat1-1* and *dgat1-2* mutants in comparison with the wild type. After the 12-h recovery period following freezing treatment, SA levels increased further and remained significantly higher in the *dgat1* mutants ($P < 0.01$; Fig. 2D).

In plant cells, the oxidative stress imposed by ROS accumulation activates the production of antioxidants, including glutathione (GSH), to maintain cellular redox homeostasis (Foyer and Noctor, 2011). Given that elevated levels of H_2O_2 were detected in *dgat1* mutants under freezing stress, we further investigated the effects of GSH application on the sensitivity of freeze-treated wild-type and *dgat1* mutant seedlings. Under normal growth conditions, the *dgat1-1* and *dgat1-2* seedlings exhibited little morphological difference from wild-type seedlings with 500 μM GSH application for 11 d (Fig. 2E). As expected, the increased sensitivities of *dgat1* mutants to the NA freezing treatment were remedied significantly by supplying GSH in Murashige and Skoog (MS) growth medium (Fig. 2, E, and F). The recovery of freezing-sensitive phenotypes of *dgat1* mutants by the addition of GSH was further confirmed by measuring the relative chlorophyll contents in the wild type and *dgat1* mutants after freezing treatment. The *dgat1* mutants accumulated significantly less chlorophyll than the wild type, but this difference was not observed when GSH was supplied (Fig. 2G).

The *dgat1* Mutants Show Decreased Expression of *CBF2* and Its Target Genes

To further elucidate the association of freezing-sensitive phenotypes of *dgat1* mutants with the CBF-dependent

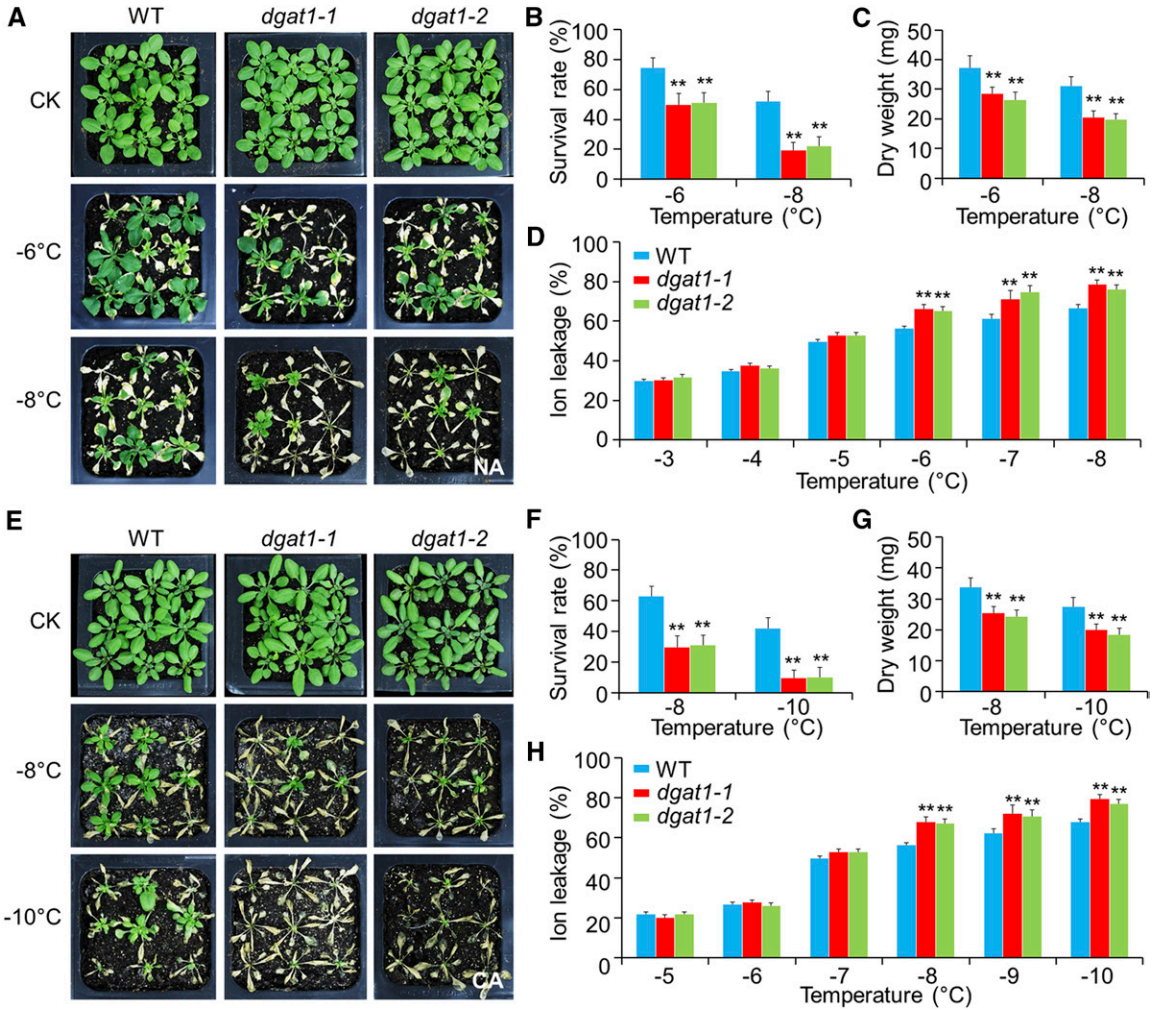

Figure 1. *dgat1* mutants display decreased freezing tolerance. A, Images of NA wild-type (WT), *dgat1-1*, and *dgat1-2* plants before (CK) and after 40 min at −6°C and −8°C freezing temperatures followed by a 5-d recovery period at normal growth conditions. B and C, Survival rate (B) and dry weight (C) of NA wild-type, *dgat1-1*, and *dgat1-2* plants after freezing treatment (−6°C and −8°C) followed by a 5-d recovery. D, Electrolyte leakage of NA wild-type, *dgat1-1*, and *dgat1-2* plants upon freezing exposure (−3°C, −4°C, −5°C, −6°C, −7°C, and −8°C). E, Images of CA wild-type, *dgat1-1*, and *dgat1-2* plants before (CK) and after 40-min treatments at −8°C and −10°C freezing temperatures followed by a 5-d recovery under normal growth conditions. F and G, Survival rate (F) and dry weight (G) of CA wild-type, *dgat1-1*, and *dgat1-2* plants after the freezing treatment (−8°C and −10°C) followed by a 5-d recovery period. H, Electrolyte leakage of CA wild-type, *dgat1-1*, and *dgat1-2* plants after freezing treatments (−5°C, −6°C, −7°C, −8°C, −9°C, and −10°C). The experiments were repeated three times independently. Data are means ± SD ($n = 3$ biological replicates). For each experiment, five independent technical replicates (grouped by three different plants) were analyzed for each genotype. Asterisks indicate significant differences from the wild type (**, $P < 0.01$, Student's *t* test).

signaling pathway, we analyzed the expression levels of *CBFs* (*CBF1*, *CBF2*, and *CBF3*) and their target genes, *COR47*, *RD29A*, and *KIN1*, by RT-qPCR. The cold-inducible expression of *CBF2* at 3, 6, 12, and 24 h, and its targets *COR47*, *RD29A*, and *KIN1* at 6, 12, and 24 h after cold treatment, were significantly lower ($P < 0.01$) in the *dgat1* mutants compared with wild-type plants (Supplemental Fig. S4). In contrast, *CBF1* and *CBF3* expression was only down-regulated in the *dgat1* mutants 3 h after cold treatment and showed similar levels to wild-type plants afterward (Supplemental Fig. S4). Therefore, the lower expression of *CBF2*, *COR47*, *RD29A*, and *KIN1* may contribute to the increased sensitivity to chilling and freezing stresses in the *dgat1* mutants.

Changes in Glycerolipid Levels in the Wild Type and *dgat1* Mutants upon Freezing Exposure

DGAT1 is a DAG acyltransferase that catalyzes the conversion of DAG to TAG in plants (Katavic et al., 1995; Routaboul et al., 1999; Zou et al., 1999; Zhang et al.,

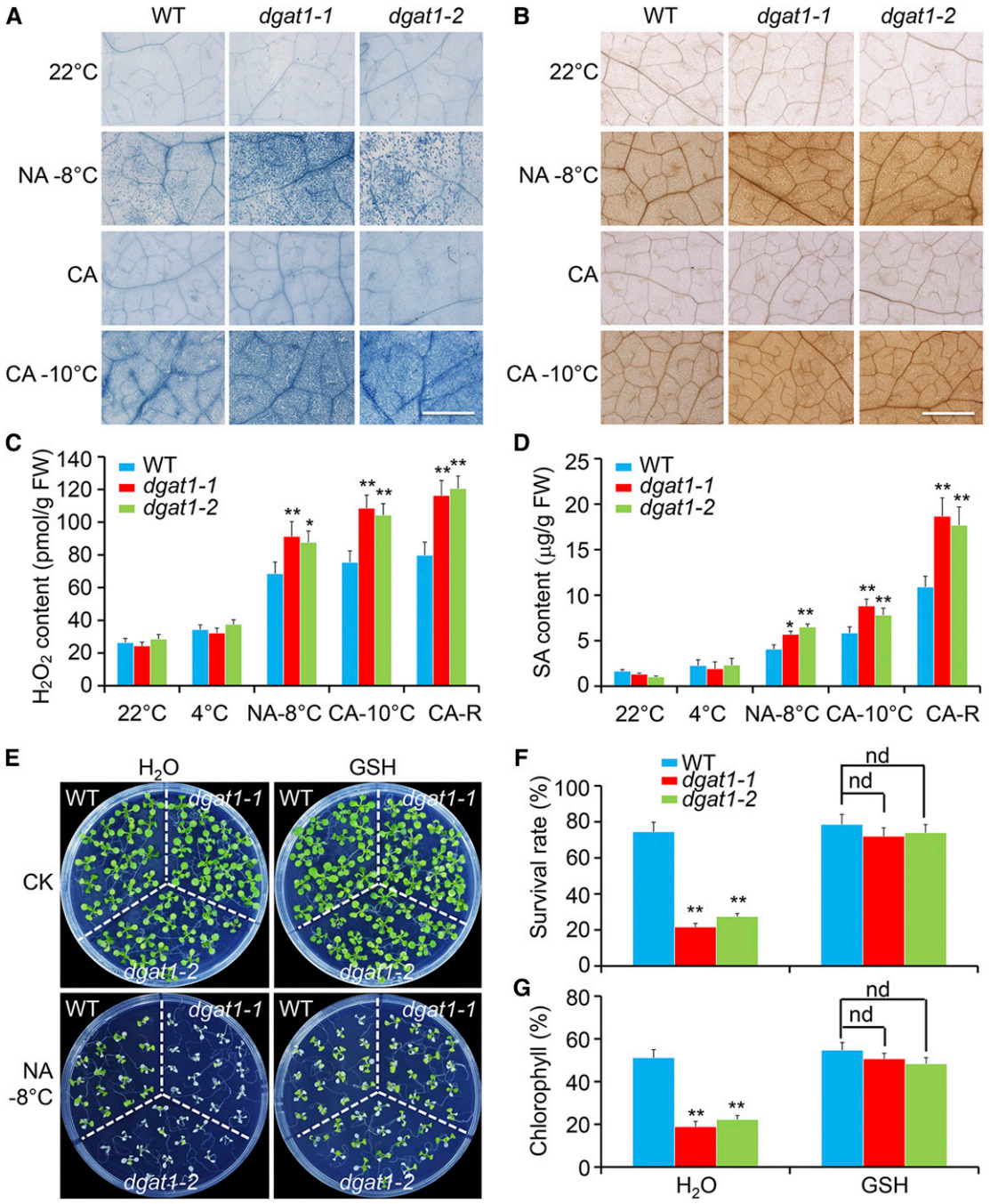

Figure 2. Cell death, H_2O_2 levels, and SA levels in the rosettes of wild-type (WT) and *dgat1* plants upon freezing treatment. A and B, Trypan Blue (A) and DAB (B) staining showing cell death and ROS accumulation in the rosettes of wild-type, *dgat1-1*, and *dgat1-2* plants before (22°C) and after treatment. Bars = 1 mm. C, H_2O_2 accumulation in the rosettes of wild-type, *dgat1-1*, and *dgat1-2* plants. FW, Fresh weight. D, SA levels in the leaves of wild-type, *dgat1-1*, and *dgat1-2* plants. Rosettes of 4-week-old wild-type, *dgat1-1*, and *dgat1-2* plants, NA or CA for 3 d, were transferred to −8°C (for NA plants) or −10°C (for CA plants) and subsequently recovered for 12 h at 4°C. Rosettes were collected for Trypan Blue staining, DAB staining, and H_2O_2 and SA content measurements. E, Phenotypes of 11-d-old wild-type, *dgat1-1*, and *dgat1-2* seedlings before (CK) and after freezing treatment (NA −8°C) and treatment with 500 μM GSH, following a 5-d recovery at normal growth conditions. F and G, Survival rate (F) and relative chlorophyll content (G) of NA wild-type, *dgat1-1*, and *dgat1-2* seedlings after medium freezing treatment (−8°C) followed by a 5-d recovery at normal growth conditions. The relative chlorophyll content under NA −8°C treatment was expressed as a percentage of the value for the same genotype grown under normal growth conditions (CK, set to 100%). nd, No significant difference. The experiments were repeated three times with more than 15 plants used for each genotype. Data are means ± SD (n = 3 biological replicates). Asterisks indicate significant differences from the wild type (**, $P < 0.01$, Student's t test).

Table I. Total lipid content in each head group class in leaves of wild-type, *dgat1-1*, and *dgat1-2* plants upon NA or CA treatment followed by freezing

The lipid contents in rosettes of plants grown at 22°C were measured as controls. Values are means ± SD (nmol mg^{-1} dry weight; $n = 4$). Significant differences between *dgat1-1* and *dgat1-2* and the wild type in each group are highlighted in boldface (*, $P < 0.05$ and **, $P < 0.01$, Student's *t* test).

Lipid Class	22°C			NA −8°C			CA −10°C		
	Wild Type	*dgat1-1*	*dgat1-2*	Wild Type	*dgat1-1*	*dgat1-2*	Wild Type	*dgat1-1*	*dgat1-2*
MGDG	204.9 ± 6.7	207.5 ± 8.5	198.7 ± 9.6	128.7 ± 7.8	134.1 ± 9.2	131.6 ± 8.8	132.8 ± 8.8	133.8 ± 10.9	128.9 ± 11.3
DGDG	39.1 ± 5.7	37.5 ± 4.6	38.3 ± 4.2	53.2 ± 5.7	50.8 ± 4.4	51.3 ± 4.9	45.4 ± 5.1	52.5 ± 3.7	50.1 ± 4.2
PG	15.5 ± 2.1	15.6 ± 1.7	15.1 ± 1.4	13.5 ± 2.8	12.7 ± 2.6	14.2 ± 3.2	14.7 ± 2.1	15.7 ± 1.8	15.9 ± 2.2
PC	15.0 ± 2.3	13.8 ± 2.7	14.4 ± 1.8	9.3 ± 1.2	8.7 ± 1.1	8.9 ± 1.1	8.7 ± 1.1	8.3 ± 0.9	8.6 ± 1.0
PE	2.5 ± 0.4	2.3 ± 0.2	2.3 ± 0.3	3.9 ± 0.2	**4.4 ± 0.2***	4.1 ± 0.3	3.5 ± 0.3	**4.0 ± 0.2***	**4.1 ± 0.2***
PI	5.8 ± 0.8	5.4 ± 0.4	4.9 ± 0.5	5.5 ± 0.7	5.9 ± 0.4	6.1 ± 0.7	5.8 ± 0.7	6.1 ± 0.6	5.7 ± 0.7
PS	0.27 ± 0.05	0.30 ± 0.06	0.32 ± 0.04	0.33 ± 0.04	0.36 ± 0.06	0.33 ± 0.03	0.31 ± 0.05	0.28 ± 0.04	0.29 ± 0.06
PA	0.07 ± 0.04	0.09 ± 0.03	0.08 ± 0.04	9.74 ± 1.1	**18.03 ± 2.7****	**17.85 ± 2.6****	11.65 ± 0.9	**23.50 ± 1.1****	**23.56 ± 1.9****
LysoPG	0.18 ± 0.03	0.26 ± 0.05	0.19 ± 0.03	0.26 ± 0.04	0.28 ± 0.02	0.26 ± 0.03	0.21 ± 0.04	0.27 ± 0.03	0.22 ± 0.02
LysoPC	0.09 ± 0.03	0.07 ± 0.02	0.06 ± 0.03	0.57 ± 0.07	0.55 ± 0.05	0.61 ± 0.05	0.61 ± 0.09	0.57 ± 0.07	0.66 ± 0.09
LysoPE	0.07 ± 0.04	0.05 ± 0.02	0.06 ± 0.01	0.52 ± 0.05	0.54 ± 0.03	0.56 ± 0.03	0.44 ± 0.06	0.48 ± 0.07	0.51 ± 0.07

2009a). Thus, we next asked whether the disruption of *DGAT1* alters the glycerolipid profiles of Arabidopsis rosettes under freezing conditions. To this end, we used electrospray ionization-tandem mass spectrometry to analyze the profiles of galactolipids and PLs in wild-type, *dgat1-1*, and *dgat1-2* rosettes under normal growth conditions (22°C) or after exposure to freezing temperatures (NA −8°C or CA −10°C). Under normal conditions (22°C), few differences were detected between the wild-type and *dgat1* plants (Table I; Fig. 3). After NA −8°C or CA −10°C treatment, the total contents of PA were significantly higher in the *dgat1* mutants compared with the wild type (Table I). When specific lipid species were analyzed, the levels of PA species, including 34:6-PA, 34:5-PA, 34:4-PA, 34:3-PA, 34:2-PA, 34:1-PA, 36:6-PA, 36:5-PA, and 36:4-PA under both NA −8°C and CA −10°C treatment, were significantly higher in *dgat1* than in wild-type rosettes ($P < 0.01$; Fig. 3). In addition, total PE levels were elevated slightly in the *dgat1* mutants under freezing treatment compared with the wild type (Table I). Specifically, the levels of 36:5-PE under NA −8°C and 34:3-PE, 34:2-PE, and 36:5-PE under CA −10°C were higher in both *dgat1-1* and *dgat1-2* mutants (Fig. 3). In addition, 36:5-PS under NA −8°C and 36:5-PS and 36:2-PS under CA −10°C increased in the *dgat1* mutants, although total PS contents showed no significant differences from the wild type in all conditions (Table I; Fig. 3).

The DGAT1-Mediated Freezing Response Requires RbohD

Previous findings suggest that PA can bind directly to the NADPH oxidase RbohD, leading to abscisic acid (ABA)-mediated ROS production and stomatal closure (Zhang et al., 2009b). Because of the elevation of H_2O_2 and PA contents in the *dgat1* mutants under freezing treatment, we proposed that higher H_2O_2 production in the *dgat1* mutants may result from the stimulation of RbohD activity by the accumulated PA. To test this possibility, we generated a *dgat1 rbohD* double mutant by crossing *dgat1-1* to the *rbohD* knockout line (Chen et al., 2015a). Phenotypic analyses showed that, upon freezing exposure, the *rbohD* single mutant exhibited improved freezing tolerance compared with the wild type (Fig. 4, A and B). In contrast to the freezing-hypersensitive phenotype of the *dgat1-1* mutant, the *dgat1 rbohD* double mutant showed similar freezing tolerance to the wild-type plants (Fig. 4, A and B), suggesting that the freezing response of *dgat1* mutants requires functional RbohD.

To determine whether the freezing-induced accumulation of PA in the *dgat1* mutants affects ROS production, we measured NADPH oxidase activity in wild-type, *dgat1-1*, *dgat1 rbohD*, and *rbohD* rosettes under normal conditions (22°C) or after NA −8°C and CA −10°C treatments. In wild-type plants, both NA and CA freezing treatments stimulated NADPH oxidase activity compared with normal conditions (Fig. 4C). Under freezing treatments, *dgat1-1* and *rbohD* mutants

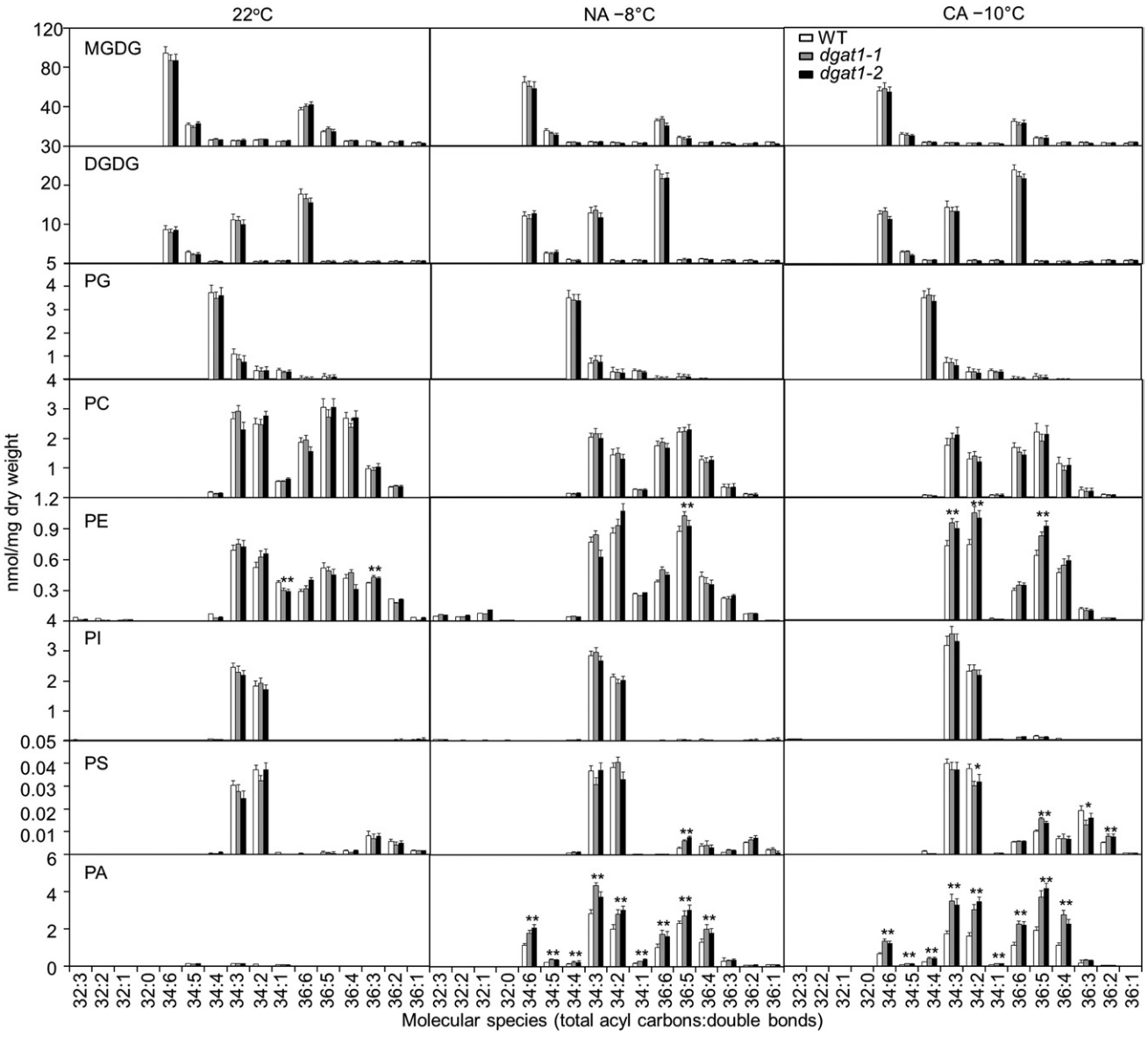

Figure 3. Lipid profiles in the rosettes of 4-week-old wild-type (WT), *dgat1-1*, and *dgat1-2* plants before (22°C) and after NA or CA treatment followed by freezing exposure (NA −8°C or CA −10°C). Alterations are shown in the compositions of galactolipids (MGDG and digalactosyldiacylglycerol [DGDG]) and PLs (Phosphatidylglycerol [PG], phosphatidylcholine [PC], phosphatidylethanolamine [PE], phosphatidylinositol [PI], phosphatidylserine [PS], and PA) of wild-type, *dgat1-1*, and *dgat1-2* rosettes before (22°C) and after NA or CA treatment followed by freezing stress (−8°C or −10°C). Values represent means ± SD ($n = 4$) of four independent samples, with each sample collected from the rosettes of three plants. Asterisks indicate significant differences from the wild type (*, $P < 0.05$ and **, $P < 0.01$, Student's *t* test).

displayed significantly higher and lower NADPH oxidase activities, respectively, than wild-type plants ($P < 0.01$; Fig. 4C). Particularly, NADPH oxidase activity in the *dgat1-1* mutant was reduced to wild-type levels by introducing the *rbohD* mutation (Fig. 4C). Moreover, the *rbohD* mutation also attenuated the accumulation of H_2O_2 under freezing treatment in the *dgat1 rbohD* double mutant relative to *dgat1-1* (Fig. 4D).

To verify whether the PA-triggered accumulation of ROS and cell death require a functional RbohD, both wild-type and *rbohD* rosettes were treated with PA or PC for 24 h, and the levels of H_2O_2 and cell death were detected by DAB and Trypan Blue staining, respectively. Application of PA, rather than PC, significantly induced H_2O_2 production and cell death in the wild-type leaves (Supplemental Fig. S5). By contrast, H_2O_2 production and cell death were abolished in the *rbohD* rosettes, suggesting that PA-promoted cell death requires a functional RbohD. Together, these results suggest

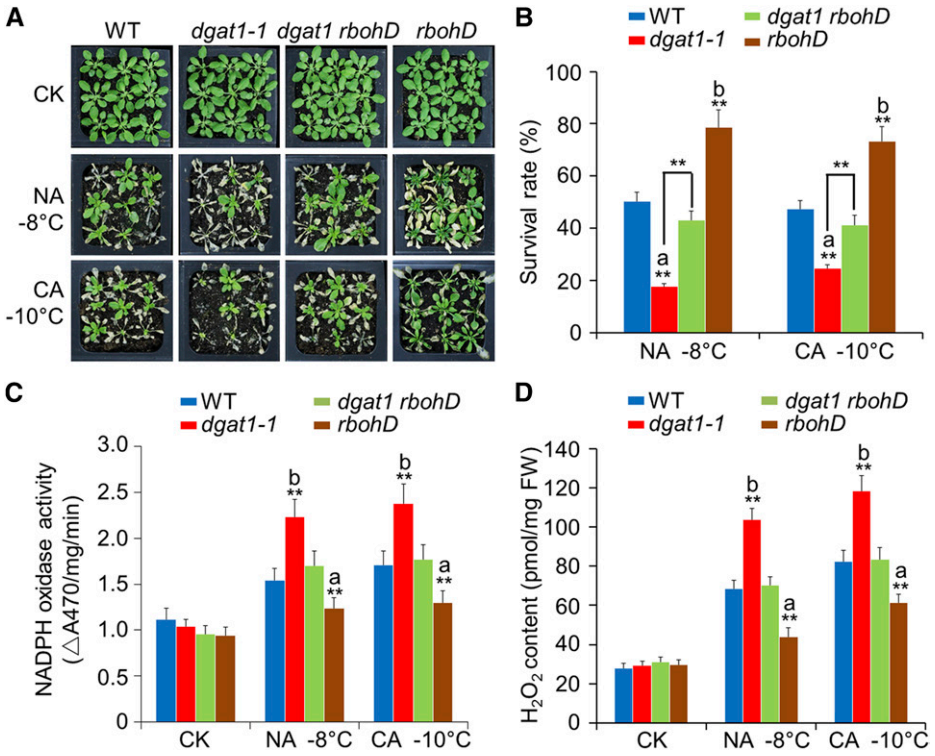

Figure 4. The increased freezing sensitivity of *dgat1* mutants requires RbohD. A, Four-week-old wild-type (WT), *dgat1-1*, *dgat1 rbohD*, and *rbohD* plants before (CK) and after freezing treatment (NA −8°C and CA −10°C) followed by a 5-d recovery period at normal growth conditions. B, Survival rate of wild-type, *dgat1-1*, *dgat1 rbohD*, and *rbohD* plants after freezing treatment (NA −8°C and CA −10°C) followed by a 5-d recovery. C and D, NADPH activity (C) and H_2O_2 levels (D) in the rosettes of wild-type, *dgat1-1*, *dgat1 rbohD*, and *rbohD* plants before and after freezing treatment (NA −8°C and CA −10°C) followed by a 5-d recovery. NADPH oxidase activity is presented as ΔA_{470} per milligram of protein per minute in C. FW, Fresh weight. Letters a and b indicate lower and higher survival rate, NADPH activity, and H_2O_2 level in the freeze-treated mutants, respectively, compared with wild-type plants. The experiments were repeated three times with more than 15 plants used for each genotype. Data are means ± SD (n = 3 biological replicates). Asterisks indicate significant differences from the wild type (**, $P < 0.01$, Student's t test).

that PA-RbohD-triggered H_2O_2 production contributes to the decreased freezing tolerance of *dgat1*.

Disruption of *DGAT1* Suppresses the Freezing-Induced Conversion of DAG to TAG

Under chilling or freezing temperatures, PA is produced through either the hydrolysis of PLs by PLDs or the phosphorylation of DAG by DGKs (Welti et al., 2002; Arisz et al., 2013). The increased accumulation of PA in *dgat1* mutants did not accompany a decrease of other PLs, such as PC, PE, PI, or PS. Therefore, we hypothesized that the loss of function of *DGAT1* might attenuate the freezing-triggered conversion of DAG to TAG, which results in PA accumulation through the DGK pathway. To test this hypothesis, we measured the levels of DAG and TAG in wild-type and *dgat1* rosettes grown under normal conditions (22°C) and after NA −8°C or CA −10°C treatment. At 22°C, the total contents of DAG and TAG showed little difference between the wild type and *dgat1* mutants (Fig. 5A). After NA −8°C or CA −10°C treatment, DAG and TAG contents were elevated substantially in the wild type compared with the untreated control (Fig. 5A). In contrast, after freezing treatments, the *dgat1* mutants showed a higher level of DAG and a lower level of TAG than the wild type (Fig. 5A). As a result, a higher DAG-TAG ratio was observed in the freeze-treated *dgat1* mutants in comparison with the wild type (Fig. 5B). Specifically, the levels of DAG with acyl chains of 18:3-16:3, 18:3-16:1, 18:3-16:0, 18:3-18:3, 18:3-18:2, 18:2-16:2, 18:2-16:1, 18:2-16:0, 18:2-18:2, and 18:1-16:3 were drastically higher in the *dgat1* mutants compared with the wild type after both NA −8°C and CA −10°C treatments (Fig. 5C). In contrast, the levels of freezing-induced TAG with acyl chains containing 16:0, 18:1, 18:2, and 18:3 were significantly lower in the *dgat1* mutants in comparison with the wild-type plants ($P < 0.01$; Fig. 5D). The higher DAG and lower TAG contents in the *dgat1* mutants under freezing stresses imply that the decreased freezing tolerance from DGAT1 loss of function is due primarily to the attenuated freezing-induced DAG-to-TAG conversion and enhanced PA production through the DGK pathway.

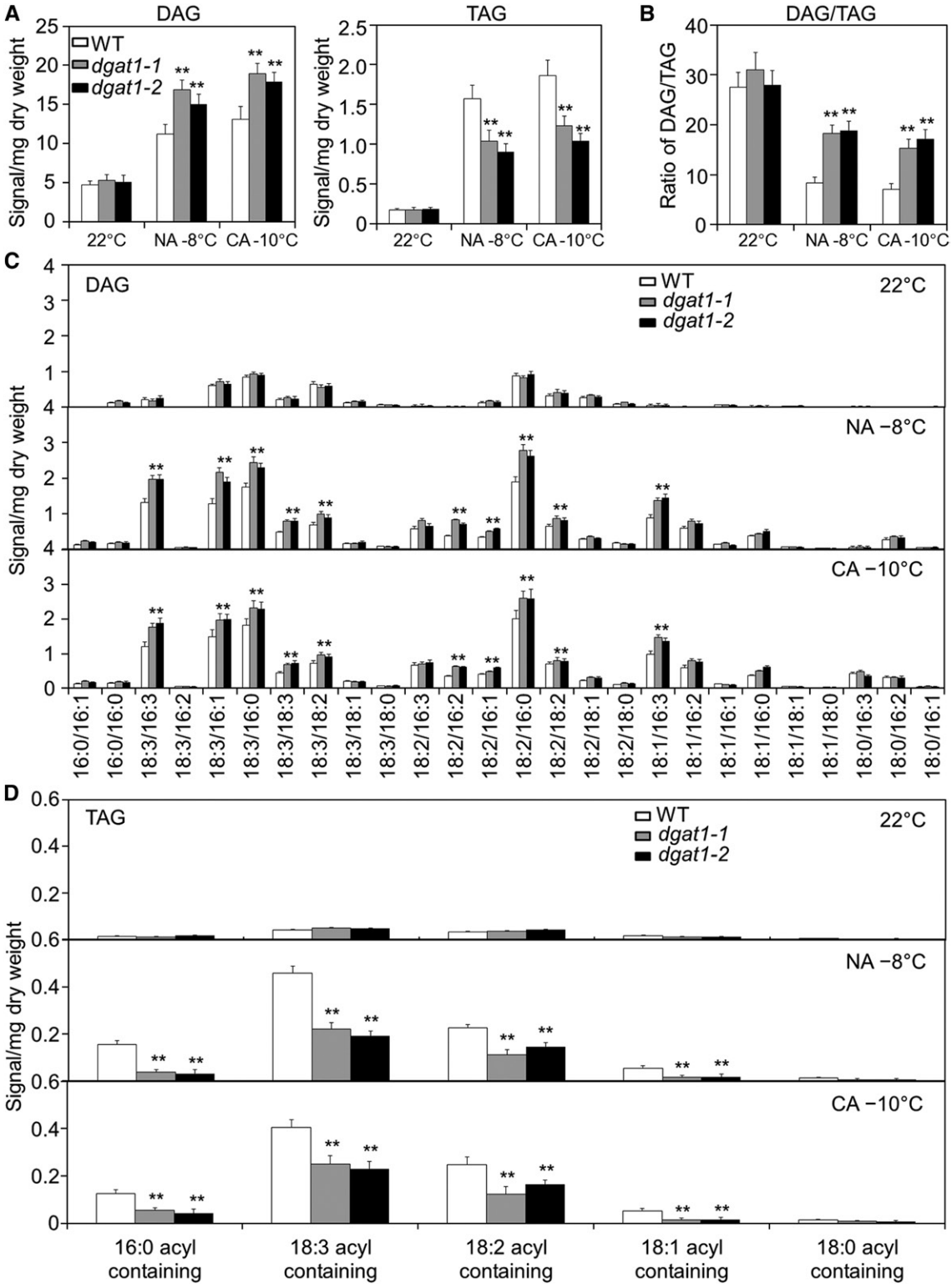

Figure 5. Profiles of DAG and TAG in rosettes of 4-week-old wild-type (WT), *dgat1-1*, and *dgat1-2* plants before (22°C) and after NA or CA treatment followed by freezing exposure (−8°C for NA and −10°C for CA). A and B, Relative levels (signal mg^{-1} dry weight) of total DAG and TAG in wild-type, *dgat1-1*, and *dgat1-2* rosettes before (22°C) and after NA or CA followed by freezing treatment. The DAG-TAG ratio of each treatment is presented in B. C and D, Molecular species of DAG (C) and TAG (D) in wild-type, *dgat1-1*, and *dgat1-2* rosettes before (22°C) and after freezing treatment (NA −8°C and CA −10°C). Data are means ± SD ($n = 4$) of four independent samples, and each sample was collected from the rosettes of three plants. Asterisks indicate significant differences from the wild type (**, $P < 0.01$, Student's t test).

Previous findings suggest that, under freezing temperatures, the increased DAG and TAG in Arabidopsis rosettes is likely due to their conversion from MGDG by SFR2 (Thorlby et al., 2004; Fourrier et al., 2008; Moellering et al., 2010). To verify the source of freezing-induced DAG and TAG, we further analyzed the levels of these two lipids in two *SFR2* knockout mutants, *sfr2-3* and *sfr2-4* (Moellering et al., 2010), under freezing conditions. We observed that, in response to freezing treatment, the total levels of DAG were significantly lower in the *sfr2* mutants compared with wild-type rosettes (Supplemental Fig. S6A). More specifically, DAG species with 16:3 and 18:3 acyl chains, which are the characteristics of MGDG acyl composition, increased significantly in the wild type but remained unchanged in the *sfr2* mutants after freezing treatment (Supplemental Fig. S6C). Consistent with the alterations of DAG, total TAG levels also showed significantly lower levels in the *sfr2* mutants compared with wild-type rosettes upon freezing exposure (Supplemental Fig. S6A). Moreover, TAG species with 18:3 acyl chain were almost absent in *sfr2* mutants after freezing treatment (Supplemental Fig. S6D). We conclude that the accumulated DAG levels under freezing temperatures are largely converted from MGDG by SFR2.

DGK2, *DGK3*, and *DGK5* Deletion Confers Enhanced Freezing Tolerance and Decreased PA Production

To investigate the potential role of DGKs in DGAT1-mediated freezing tolerance, we first analyzed the expression levels of *DGKs* and *PLDs* in wild-type and *dgat1* plants in response to cold treatments. The transcripts of all *DGK* genes were up-regulated by brief exposure to chilling temperatures (Fig. 6A), which confirmed previous findings (Arisz et al., 2013; Chen et al., 2015b). We also observed that the expression levels of *DGK1*, *DGK2*, *DGK3*, and *DGK5* were further elevated by freezing treatment and postfreezing recovery (Fig. 6A). Moreover, the expression levels of *DGK2*, *DGK3*, and *DGK5* were significantly higher in both *dgat1-1* and *dgat1-2* mutants at 12, 24, and 72 h after 4°C exposure, after freezing treatments, and following the postfreezing recovery period compared with the wild-type plants ($P < 0.01$; Fig. 6A). In contrast, transcript levels of *DGK1*, *DGK4*, and *DGK6* were up-regulated in the wild type and *dgat1* mutants under freezing and postfreezing conditions, but *DGK1* expression at 12 and 24 h and *DGK4* and *DGK6* expression at 12 h were higher in the mutants than in the wild type (Fig. 6A). In comparison, the cold-induced expression levels of *PLDα1* and *PLDδ*, used as controls, showed no significant difference between the wild-type and *dgat1* plants in response to cold treatments (Fig. 6A). These results suggest that *DGK2*, *DGK3*, and *DGK5* may share a predominant role in the DGAT1-mediated freezing response.

Under freezing temperatures, MGDG is converted to oligogalactolipids and DAG; the latter is likely released to the cytosol during freezing-induced membrane shrinkage (Moellering et al., 2010; Moellering and Benning, 2011). To determine this possibility, we further examined the subcellular localization of DGK2, DGK3, and DGK5 proteins. By expression in Arabidopsis protoplasts, we observed that all of the DGK2-GFP, DGK3-GFP, and DGK5-GFP fusions were localized in the cytosol (Supplemental Fig. S7), suggesting that they are available for the cytosolic conversion of MGDG-derived DAG to PA.

The functions of DGKs in freezing tolerance were validated by analyses of the *DGK2*, *DGK3*, and *DGK5* knockout mutants. To this end, lines with T-DNA insertions in *DGK2*, *DGK3*, and *DGK5* were identified. The transcripts of *DGK2*, *DGK3*, and *DGK5* were undetectable in the respective *dgk2-1*, *dgk3-1*, and *dgk5-1* lines (Supplemental Fig. S8), suggesting that all lines contain knockout alleles. Phenotypic analyses showed that, under normal growth conditions, the 4-week-old *dgk2-1*, *dgk3-1*, and *dgk5-1* mutants exhibited little morphological difference from wild-type plants (Fig. 6B). However, when the NA and CA plants were exposed to freezing temperatures (−8°C or −10°C), all the *dgk* mutants showed enhanced tolerance to freezing stress (Fig. 6B). The freezing-tolerant phenotypes of the *dgk* mutants were further confirmed by higher survival rates and dry weights than wild-type plants during NA −8°C or CA −10°C followed by a 5-d recovery (Fig. 6C).

To evaluate the function of DGKs in the phosphorylation of DAG for PA synthesis under freezing conditions, we next analyzed the lipid profiles in wild-type, *dgk2-1*, *dgk3-1*, and *dgk5-1* rosettes under normal growth conditions (22°C) or after exposure to freezing temperatures (NA −8°C or CA −10°C). Under normal growth conditions (22°C), the rosettes of wild-type and *dgat1* plants showed few significant differences in either galactolipids or PLs (Fig. 7A; Supplemental Fig. S9). After NA −8°C or CA −10°C treatment, the total contents of PC, PE, PI, and PS declined in both the wild type and *dgk* mutants (Fig. 7A; Supplemental Fig. S9). As expected, the contents of PA were significantly lower in the *dgk* mutants compared with the wild type (Fig. 7A). Particularly, the levels of PA species, including 34:6-PA, 34:3-PA, 34:2-PA, 34:1-PA, 36:6-PA, 36:5-PA, 36:4-PA, and 36:3-PA, were significantly lower in the *dgk* mutants compared with wild-type rosettes under NA −8°C and/or CA −10°C treatments (Fig. 7B). As a result of the attenuated freezing-inducible PA accumulation, the *dgk* mutants showed inhibited NADPH oxidase activity and lower H_2O_2 production in comparison with wild-type plants (Fig. 7, C and D). Compared with wild-type plants, all the single *dgk2-1*, *dgk3-1*, and *dgk5-1* mutants showed enhanced freezing-tolerant phenotypes (Fig. 6B), decreased PA level (Fig. 7, A and B), and reduced H_2O_2 production (Fig. 7D) in response to freezing stress. Therefore, DGK2, DGK3, and DGK5 proteins are predominantly functional in converting DAG to PA upon freezing exposure.

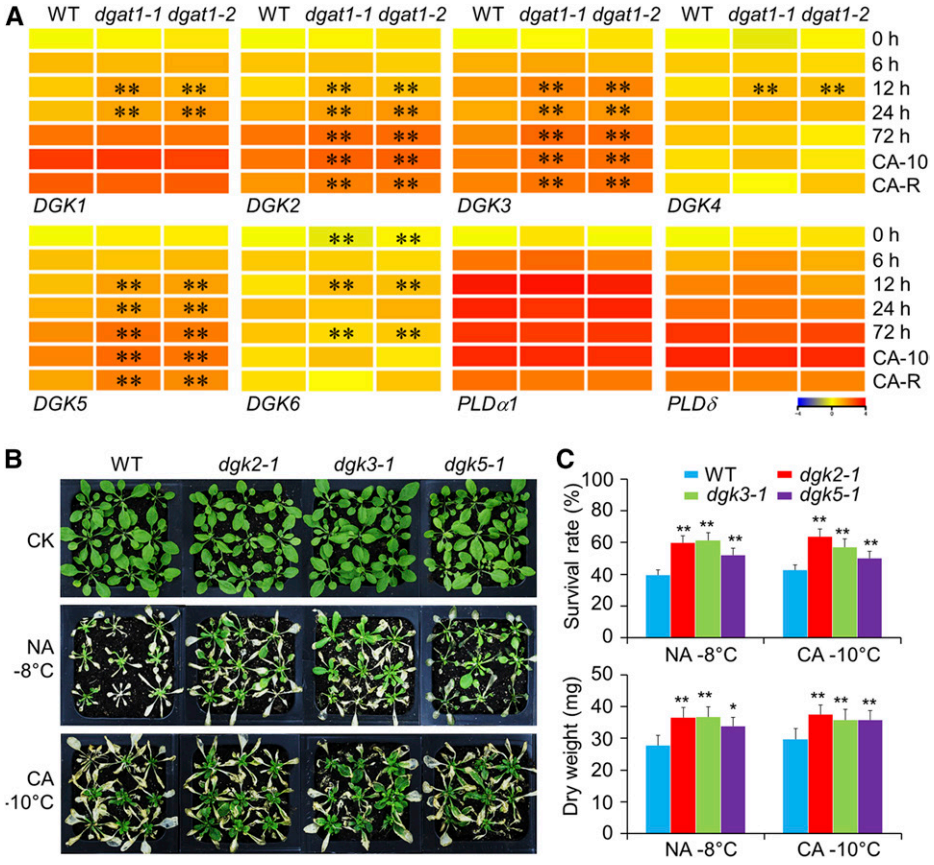

Figure 6. Knockout of *DGK2*, *DGK3*, and *DGK5* confers enhanced freezing tolerance. A, Expression profiles of cold-responsive *DGKs* and *PLDs* in wild-type (WT), *dgat1-1*, and *dgat1-2* plants under cold (4°C) or freezing (−10°C) temperatures followed by recovery. Rosettes of 4-week-old wild-type, *dgat1-1*, and *dgat1-2* plants treated at 4°C for 0, 6, 12, 24, and 72 h, freezing (−10°C) for 40 min (CA −10), and following recovery at 4°C for 6 h (CA-R) were collected for total RNA extraction. Hierarchical cluster analyses were used in the transcript levels of six *DGKs* (*DGK1*, *DGK2*, *DGK3*, *DGK4*, *DGK5*, and *DGK6*), *PLDα1*, and *PLDδ* determined by RT-qPCR. Three biological replicates were conducted with similar results, and representative data from one experiment are shown. Data are means ± SD ($n = 3$) of three technical replicates. The relative gene expression values were plotted with the heatmap 2.0 package in R, with red and blue colors representing up- and down-regulation, respectively. Asterisks indicate significant differences in *dgat1-1* and *dgat1-2* plants compared with the wild type (**, $P < 0.01$, Student's *t* test). B, NA and CA wild-type, *dgk2-1*, *dgk3-1*, and *dgk5-1* seedlings before (CK) and after freezing treatment (NA −8°C or CA −10°C) followed by a 5-d recovery period at normal growth conditions. C, Survival rate and dry weight of NA and CA wild-type, *dgk2-1*, *dgk3-1*, and *dgk5-1* plants after freezing treatment (NA −8°C or CA −10°C) followed by a 5-d recovery period.

DISCUSSION

Arabidopsis DGAT1 acts as an acyl-CoA:DAG acyltransferase in converting DAG to TAG during seed oil deposition (Katavic et al., 1995; Routaboul et al., 1999; Zou et al., 1999; Zhang et al., 2009a). Previous findings suggest that the freezing-induced accumulation of the PL PA forms a destabilized H_{II}-type phase with MGDG or DAG, which damages cell membrane integrity under freezing temperatures, thus attenuating the plant tolerance to such stresses (Steponkus, 1984; Uemura et al., 1995; Thomashow, 1999; Welti et al., 2002; Moellering et al., 2010; Moellering and Benning, 2011). Recent studies reveal that, upon freezing exposure, the galactolipid MGDG is converted to oligogalactolipids and DAG, the latter of which is likely further catalyzed to TAG for membrane stabilization (Moellering et al., 2010; Moellering and Benning, 2011). In response to chilling or freezing, DAG also can be phosphorylated by DGKs to produce PA (Gómez-Merino et al., 2004; Arisz et al., 2013; Chen et al., 2015b). These findings indicate that DGATs and DGKs potentially function in regulating lipid remodeling in the plant response to low temperatures. However, how plant cells integrate the dynamics of these lipids to mediate sensitivity to cold stresses remains unknown.

Here, we presented several lines of evidence to support the idea that Arabidopsis DGAT1 and DGK2/3/5 contribute to the freezing response by modulating the homeostasis of DAG, TAG, and PA. First, the transcript of *DGAT1* was induced by chilling treatment, and the *DGAT1* null mutants, *dgat1-1* and *dgat1-2*, were more

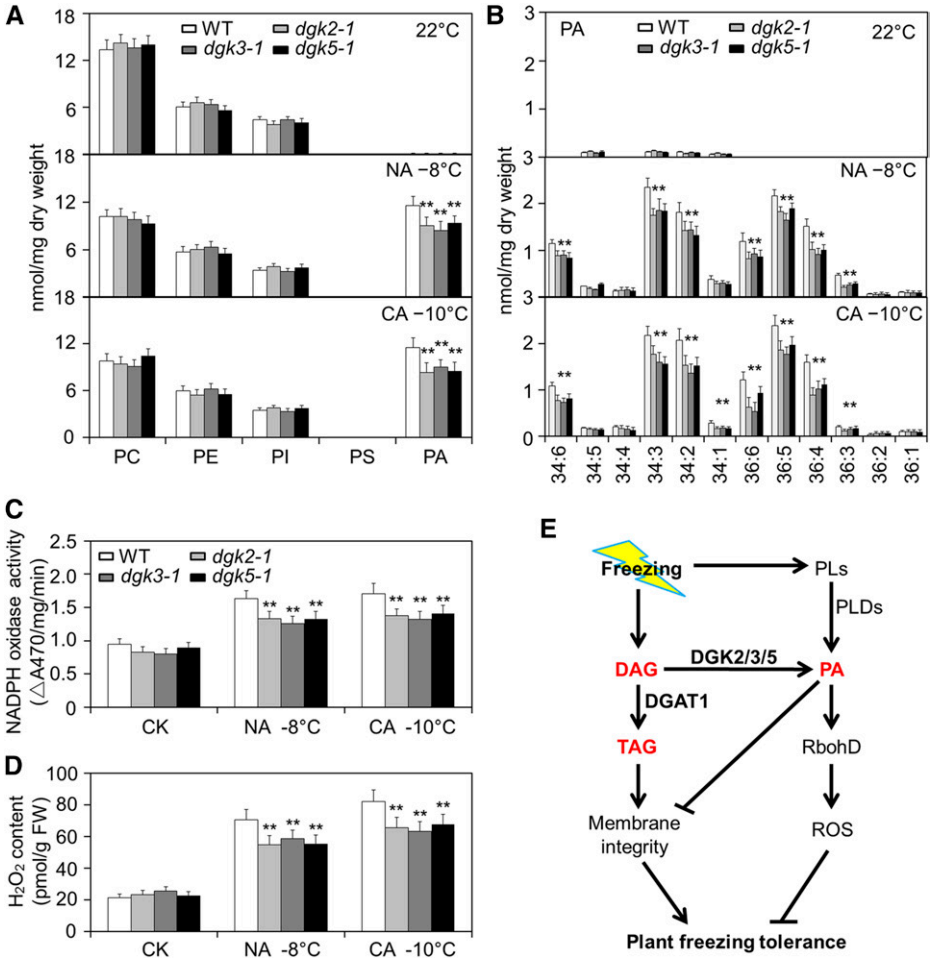

Figure 7. Total lipids and PA species of 4-week-old wild-type (WT), *dgk2-1*, *dgk3-1*, and *dgk5-1* plants before (22°C) and after NA or CA treatment following freezing exposure (NA −8°C or CA −10°C). A, Alteration in the compositions of PLs (PC, PE, PI, PS, and PA) of wild-type, *dgk2-1*, *dgk3-1*, and *dgk5-1* rosettes before (22°C) and after NA or CA following freezing stress (−8°C or −10°C). B, Concentrations of PA species of wild-type, *dgk2-1*, *dgk3-1*, and *dgk5-1* rosettes before (22°C) and after NA or CA following freezing stress (−8°C or −10°C). C and D, NADPH activity (C) and H_2O_2 levels (D) of wild-type, *dgk2-1*, *dgk3-1*, and *dgk5-1* plants before (CK) and after freezing treatment (NA −8°C or CA −10°C). NADPH oxidase activity is presented as ΔA_{470} per milligram of protein per minute. FW, Fresh weight. E, A working model showing the role of DGAT1 in the plant response to freezing by modulating DAG homeostasis and ROS production.

sensitive to chilling and freezing stresses (Fig. 1; Supplemental Figs. S1 and S3). Second, the *dgat1* mutants showed lower levels of cold-inducible expression of *CBF2* and its regulons (Supplemental Fig. S4). Third, the decreased freezing tolerance of *dgat1* mutants was associated with the enhanced accumulation of ROS under freezing treatment, which required a functional RbohD (Figs. 2 and 4). Fourth, lipid profiling revealed that, in response to freezing temperatures, the *dgat1* mutants showed significantly higher levels of PA and DAG but significantly lower levels of TAG compared with wild-type plants (Figs. 3 and 5). Finally, knocking out *DGK2*, *DGK3*, and *DGK5* reduced DAG-derived PA production and improved plant tolerance to freezing stress (Figs. 6 and 7). Taken together, our findings reveal that DAG is an essential substrate for the DGAT1 and DGK2/3/5 enzymes in the remodeling of cold-responsive lipids in Arabidopsis.

When temperatures decline as low as 0°C, ice crystals form in the extracellular space, leading to dehydration and plant cell damage (Thomashow, 1999; Yamaguchi-Shinozaki and Shinozaki, 2006). Under chilling and freezing conditions, plants have developed several physiological and biochemical strategies, including remodeling of the plastidic and extraplastidic membrane lipid compositions, to prevent cold-induced cell damage (Uemura et al., 1995; Welti et al., 2002; Li et al., 2004, 2008; Moellering et al., 2010; Chen and Thelen, 2013). For instance, upon cold exposure, the amounts of unsaturated fatty acids or PLs increase drastically, thus enhancing membrane fluidity and integrity. In contrast, the freezing-inducible accumulation

of lipids with small or lacking head groups, such as MGDG, DAG, and PA, tends to form a nonlamellar H_{II}-type phase, which results in the shrinkage of membrane structure and membrane ionic leakage (Kuiper, 1970; Verkleij et al., 1982; Welti et al., 2002; Moellering et al., 2010).

Previous studies reveal that Arabidopsis SFR2, a galactolipid:galactolipid galactosyltransferase, catalyzes the freezing-inducible conversion of MGDG to DGDG and other oligogalactolipids in the chloroplast outer envelope. As a result, it reduces inverted H_{II}-type structure formation and improves plant freezing tolerance (Thorlby et al., 2004; Fourrier et al., 2008; Moellering et al., 2010). Furthermore, the freezing-hypersensitive mutant *sfr2* displays significantly lower TAG levels compared with wild-type plants (Supplemental Fig. S6; Moellering et al., 2010). Consistent with this, our recent work shows that mutants of three lipase-like regulators in the SA signaling pathway, *sag101*, *eds1*, and *pad4*, exhibit enhanced freezing tolerance, along with lower DAG and higher TAG levels under freezing treatments (Chen et al., 2015b). These findings suggest that, by modulating cell membrane stability and fluidity, the ratio of DAG to TAG lipids represents an important mechanism in the regulation of plant freezing response. The *dgat1* mutants were hypersensitive to chilling and freezing (Fig. 1; Supplemental Fig. S3) and showed elevated levels of freezing-inducible DAG but lower TAG levels (Fig. 5). This result provides direct genetic evidence to show the predominant functions of DGAT1 in catalyzing the conversion of DAG to TAG in response to freezing. It is conceivable that, under freezing exposure, the DGAT1-mediated conversion of DAG to the more neutral lipid TAG acts as a protective strategy for enhancing plant tolerance to freezing stresses. Interestingly, PDAT1, another DAG acyltransferase that catalyzes the DAG-to-TAG conversion in Arabidopsis, is involved in TAG production when plants suffer heat stress (Mueller et al., 2017), suggesting that DGAT1 and PDAT1 play primary roles in the plant responses to these different abiotic stresses.

In addition to MGDG and DAG, the lipid molecule PA can form a nonlamellar lipid structure under freezing conditions, which confers increased sensitivity to cold stresses in Arabidopsis (Wang, 2004; Browse, 2010). Freezing-induced PA production can be derived from either the PLD pathway by hydrolysis of PLs or the DGK pathway by phosphorylation of DAG (Arisz et al., 2013). In Arabidopsis, two PLDs, PLDα1 and PLDδ, play distinct roles in the regulation of plant tolerance to freezing (Welti et al., 2002; Li et al., 2004; Rajashekar et al., 2006). In particular, knockout of *PLDα1* reduces the hydrolysis of PLs to PA and leads to enhanced tolerance to freezing (Welti et al., 2002; Rajashekar et al., 2006). However, the *PLDδ* null mutants show increased sensitivity to freezing, and *PLDδ* overexpressors show the opposite phenotype (Li et al., 2004). A possible explanation is that PLDα1-mediated PA accumulation can activate RbohD and facilitate H_2O_2 production, whereas PLDδ is likely involved in ROS clearance (Zhang et al., 2003, 2009b). In this study, we found that, in the freeze-treated *dgat1* mutants, the transcripts of *DGK2*, *DGK3*, and *DGK5* were elevated compared with wild-type plants (Fig. 6A). Moreover, disruption of *DGK2*, *DGK3*, and *DGK5* conferred enhanced freezing tolerance (Fig. 6B). By lipid profiling analyses, we further revealed that these three DGKs contributed redundantly to the freezing-inducible accumulation of PA, as indicated by the reductions in PA in the *dgk* mutants upon freezing exposure (Fig. 7, A and B). Therefore, we presented strong evidence to link DGK-catalyzed PA production to the DGAT1-mediated DAG-to-TAG conversion pathway in plant responses to freezing stress (Fig. 7E). Under freezing temperatures, DAG likely functions as a common substrate in balancing the downstream actions of DGAT1 and DGKs to produce the neutral TAG and polar PA, two lipids that play opposite roles in maintaining cell membrane integrity under freezing treatment. Thus, the DGK pathway functions either as a parallel mechanism or as a complementary mechanism to that of PLDs to induce PA production in response to cold stresses.

ROS are important second messengers for the regulation of plant adaption to various environmental cues, including cold temperatures (Apel and Hirt, 2004; Laloi et al., 2004). Particularly, the activities of several key enzymes in the MAPK signaling cascade, such as MEKK1-MKK1/2, are ROS responsive. In the Arabidopsis response to ABA, MKK1 directly regulates the expression of the reduction enzyme CAT1 and determines the cellular redox homeostasis (Xing et al., 2008). In contrast, MKK2 mediates plant tolerance to cold and salt stresses (Teige et al., 2004; Xing et al., 2008; Jammes et al., 2009). More recent studies reveal that two downstream ROS-responsive MPK kinases, MPK3 and MPK6, are involved in cold responses by modulating the protein stability of ICE1 (Li et al., 2017; Zhao et al., 2017), suggesting that the direct regulation of key components in cold signaling involves ROS. The increased ROS production in the *dgat1* mutants (Fig. 2, B and C) is possibly associated with the enhancement of MPK3 and MPK6 activity, leading to the degradation of ICE1. *CBF2* is one of the downstream targets of ICE1 (Chinnusamy et al., 2003; Ding et al., 2015); this may explain why the transcript levels of *CBF2* and its regulons, *COR47*, *RD29A*, and *KIN1*, were significantly lower in *dgat1* mutants than in the wild type under chilling conditions (Supplemental Fig. S4). Furthermore, increasing evidence indicates that a plant's tolerance to freezing stresses is tightly associated with its intracellular ROS level (Iba, 2002), as the accumulation of ROS can trigger irreversible oxidative damage and cause cell death (Apel and Hirt, 2004). In particular, two mutants of *LESION SIMULATING DISEASE RESISTANCE1* (*LSD1*) display chilling-sensitive phenotypes and elevated H_2O_2 levels, which can be fully suppressed by mutation of *EDS1* or *PAD4* in the *lsd1* background, indicating that LSD1 may function in plant cold responses by modulating ROS levels (Huang

et al., 2010). In Arabidopsis, ROS are primarily generated by the action of the NADPH oxidases RbohD and RbohF (Kaur et al., 2014). Previous studies suggest that PA can interact with RbohD and stimulate its activity, which facilitates ABA-responsive stomatal closure, indicating that PA is a lipid activator for RbohD-mediated ROS production (Zhang et al., 2009b). We further observed that the freezing-induced accumulation of PA in *dgat1* was associated with elevated H_2O_2 contents (Figs. 2 and 3), suggesting that PA likely contributes to ROS production by activating RbohD activity in response to freezing. Consistent with this, we found that knocking out *RbohD* in the *dgat1-1* background attenuated the increased sensitivity and enhanced H_2O_2 production upon freezing exposure (Fig. 4).

CONCLUSION

Our results demonstrate that freezing can rapidly stimulate the accumulation of DAG in Arabidopsis (Fig. 7E), possibly through the conversion of MGDG by the galactolipid-remodeling enzyme SFR2 or the hydrolysis of polyphosphoinositides by PLCs (Moellering et al., 2010; Arisz et al., 2013). In response to freezing, DGAT1 predominantly functions in catalyzing the subsequent conversion of DAG to TAG, preventing the formation of the destabilized H_{II}-type phase, as a protective mechanism to improve plant tolerance to such stresses (Fig. 7E). Freezing also induces the hydrolysis of PLs to produce PA (Welti et al., 2002; Li et al., 2004; Rajashekar et al., 2006). The elevation of PA may either disrupt membrane permeability or stimulate RbohD activity for ROS production and subsequently increase plant sensitivity to freezing (Fig. 7E). In parallel with the PLD pathway, cold-inducible DGK2/3/5 also contribute to PA generation by phosphorylating DAG (Fig. 7E). Therefore, it is conceivable that DAG may function as a common substrate necessary for both DGAT1- and DGK2/3/5-mediated TAG and PA production, respectively, the balance of which determines plant survival during freezing stress. The dynamic remodeling of DAG, TAG, and PA lipids is likely an important protective strategy enhancing plant survival of freezing temperatures.

MATERIALS AND METHODS

Plant Materials, Growth Conditions, and Treatments

The Arabidopsis (*Arabidopsis thaliana*) ethyl methanesulfonate-generated mutant *dgat1-1* (CS3861) and T-DNA insertional mutant *dgat1-2* (SALK_039456) were obtained from the Arabidopsis Biological Resource Center (http://www.arabidopsis.org). Characterization of the *dgat1-1* homozygous mutant was carried out following Zou et al. (1999). For identification of the T-DNA insertion site in the *dgat1-2* mutant, the *DGAT1*-specific primers XS1844/XS1845 and the T-DNA left border primer LBa1 (Supplemental Table S1) were used for PCR amplification. The *dgk2-1* (SAIL 718_G03), *dgk3-1* (SALK_082600), and *dgk5-1* (SAIL 1212_E10) mutants were identified by PCR using primers (Pa/Pb and Pb/LB1 for *dgk2-1*, Pc/Pd and Pd/LBa1 for *dgk3-1*, and Pe/Pf and Pf/LB1 for *dgk5-1*).

Seeds of Arabidopsis wild type (ecotype Columbia-0) and mutants were surface sterilized with 20% bleach (v/v) containing 0.1% Tween 20 (v/v) for 20 min and then washed three times with sterilized water followed by sowing on MS medium supplemented with 1% Suc. Seeds were dark treated at 4°C for 3 d and subsequently transferred to a plant growth room under a 16-h-light (23°C)/8-h-dark (21°C) cycle. After germination for 10 d, the seedlings were transplanted to soil in the plant growth room until treatment.

Chilling and freezing treatments were carried out as described previously (Chen et al., 2008) with minor modifications. For cold acclimation, 4-week-old plants were transferred from the growth room to a cold chamber (4°C) for 3 d of acclimation under a normal light/dark cycle. For the freezing treatment, all 4-week-old NA or CA soil-grown plants or 11-d-old seedlings grown on MS medium plates were transferred to a growth chamber (Blue Pard LRH-250CA) with temperatures reduced steadily from 4°C to −2°C (2°C h^{-1}). Ice crystals were then placed on the soil or plates to avoid supercooling when the temperature reached −2°C. The temperature remained at −2°C for 2 h and continued to lower until reaching the final temperatures. After staying at the final temperatures (−6°C and −8°C for NA plants, −8°C and −10°C for CA plants) for 40 min, plants or seedlings were thawed overnight at 4°C. Plants were photographed after a 5-d recovery under normal growth conditions. For GSH application experiments, seeds were sown on MS medium plates containing 500 μM GSH or MS medium plates as controls for 11 d and then subjected to freezing treatment.

Electrolyte Leakage Measurement

Measurements of ionic leakage were conducted as described by Chen et al. (2008). Rosettes of plants were collected after NA or CA freezing treatments at the indicated times and thawed at 4°C overnight. Ionic leakage was measured using a conductivity meter (Mettler Toledo S220-USP/EP). The leaked ionic strength and total ionic strength were recorded for calculation of relative ionic leakage rates.

Total RNA Extraction and RT-qPCR

TRIzol (Invitrogen) was used for total RNA extraction according to the manufacturer's recommendations. Reverse transcription was performed using the PrimeScript RT reagent kit with gDNA Eraser (Takara) to synthesize first-strand cDNA from 2 μg of total RNA. qPCR was performed by the SYBR Green method using the StepOnePlus Real-Time PCR system (Applied Biosystems) in 96-well blocks. The cycle threshold (Ct) value of each sample was calculated using the $2^{-\Delta\Delta Ct}$ method (Livak and Schmittgen, 2001). The RT-qPCR primers used are listed in Supplemental Table S1. All RT-qPCRs were performed using total RNA samples isolated from three independent replicate samples with similar results.

Trypan Blue and DAB Staining

Trypan Blue and DAB staining were carried out as described previously (Xiao and Chye, 2011). Briefly, rosettes from NA and CA freezing plants were collected and boiled in Trypan Blue staining buffer for 1 min followed by incubating at room temperature for 10 min. Then, the leaves were transferred to tubes containing 70% chloral hydrate (w/v) for destaining. For DAB staining, the collected leaves were immersed in 1 mg mL^{-1} DAB staining buffer (pH 3.8) for 5 h in the dark. Ethanol (95%) was boiled and used for chlorophyll clearing afterward.

Measurement of H_2O_2 and Chlorophyll Contents

The measurement of H_2O_2 contents was carried out as described by Yuan et al. (2017) using the Amplex Red Hydrogen Peroxide/Peroxidase Assay Kit (Molecular Probes). Briefly, rosettes from NA and CA freezing plants were ground in liquid nitrogen, and 200 mL of reaction buffer was used for H_2O_2 extraction. A microplate reader (Tecan) was employed to detect the absorbance of H_2O_2 at 560 nm. The H_2O_2 concentration was calculated using a standard curve. Chlorophyll was extracted from Arabidopsis rosettes using 1 mL of *N*,*N*-dimethylformamide (Sigma; D4551) and kept at 4°C in the dark for 2 d. Absorbance at 664 and 647 nm was recorded. Total chlorophyll was calculated as described by Thompson et al. (2005). The chlorophyll contents of wild-type samples from normal growth conditions were set to 100%, and the relative chlorophyll contents in other samples were calculated accordingly.

Lipid Profiling

Total lipid extraction was performed as described previously (Welti et al., 2002). The profiles of membrane lipids were determined by electrospray ionization-tandem mass spectrometry as described previously (Xiao et al., 2010). Data shown in this study are means with SD from four independent samples, and each sample was pooled from the rosettes of five plants. DAG and TAG levels were separated and quantified following Peters et al. (2014).

Measurement of NADPH Oxidase Activity

The plasma membrane was isolated according to Qiu et al. (2002). NADPH oxidase activity measurements were conducted following Zhang et al. (2009b). Briefly, membrane vesicles were resuspended in 50 mM Tris-HCl buffer (pH 7.5). Then, the solution was mixed with the reaction buffer containing 50 mM Tris-HCl (pH 7.5) and 0.5 mM reduction of the tetrazolium dye, XTT. Fifty micromolar NADPH was added to initiate the reaction. After incubation at room temperature for 10 min, XTT formazan production at A_{470} was detected using a microplate reader (Tecan). NADPH activity was represented as ΔA_{470} per milligram of protein per minute.

Plasmid Construction, Transient Expression, and Microscopy Analyses

To construct the DGK2-GFP, DGK3-GFP, and DGK5-GFP vectors, full-length coding sequences of *DGK2*, *DGK3*, and *DGK5* were inserted into *Bam*HI-digested pUC119 and fused with the N terminus of eGFP. Transient expression assays in Arabidopsis protoplasts were carried out according to Qi et al. (2017). Briefly, protoplasts from 4-week-old wild-type rosettes were isolated and transfected with DGK2-GFP, DGK3-GFP, and DGK5-GFP vectors. Protoplasts were incubated for 12 h, and GFP signal was detected by confocal microscopy.

Accession Numbers

The sequence data discussed in this article can be found in the Arabidopsis Genome Initiative database under the following accession numbers: *DGAT1* (AT2G19450), *PDAT1* (AT5G13640), *CBF1* (AT4G25490), *CBF2* (AT4G25470), *CBF3* (AT4G25480), *COR47* (AT1G20440), *RD29A* (AT5G52310), *KIN1* (AT5G15960), *DGK1* (AT5G07920), *DGK2* (AT5G63770), *DGK3* (AT2G18730), *DGK4* (AT5G57690), *DGK5* (AT2G20900), *DGK6* (AT4G28130), *PLDα1* (AT3G15730), *PLDδ* (AT4G35790), *SFR2* (AT3G06510), and *RbohD* (AT5G47910).

Supplemental Data

The following supplemental materials are available.

Supplemental Figure S1. Expression patterns of *DGAT1* and *PDAT1* under cold stress (4°C).

Supplemental Figure S2. Identification of *dgat1* mutants.

Supplemental Figure S3. *DGAT1* knockout mutants show increased sensitivity to chilling stress.

Supplemental Figure S4. Cold-inducible expression of *CBFs* and their regulons in the wild type and *dgat1* mutants.

Supplemental Figure S5. PA-induced H_2O_2 production and cell death require RbohD.

Supplemental Figure S6. Profiles of DAG and TAG in rosettes of 4-week-old wild type, *sfr2-3*, and *sfr2-4* before (22°C) and after NA or CA treatment followed by freezing exposure (−8°C for NA and −10°C for CA).

Supplemental Figure S7. DGK2-GFP, DGK3-GFP, and DGK5-GFP fusions are localized in the cytosol.

Supplemental Figure S8. Identification of *dgk2-1*, *dgk3-1*, and *dgk5-1* mutants.

Supplemental Figure S9. Lipid profiles in the rosettes of 4-week-old wild type, *dgk2-1*, *dgk3-1*, and *dgk5-1* before (22°C) and after NA or CA treatment following freezing exposure (NA −8°C or CA −10°C).

Supplemental Table S1. Primer sequences used in this study.

ACKNOWLEDGMENTS

We thank the Arabidopsis Biological Resource Center for providing us the *dgat1-1*, *dgat1-2*, *dgk2-1*, *dgk3-1*, and *dgk5-1* mutant seeds, H.B. Wang (Sun Yat-sen University) for the *rbohD* seeds, and H.B. Gao (Beijing Forestry University) for the *sfr2-3* and *sfr2-4* seeds. We also thank M. Roth and R. Welti (Kansas Lipidomics Research Center) for conducting lipid profiling.

Received May 3, 2018; accepted May 24, 2018; published May 31, 2018.

LITERATURE CITED

Apel K, Hirt H (2004) Reactive oxygen species: metabolism, oxidative stress, and signal transduction. Annu Rev Plant Biol **55**: 373–399

Arisz SA, van Wijk R, Roels W, Zhu JK, Haring MA, Munnik T (2013) Rapid phosphatidic acid accumulation in response to low temperature stress in *Arabidopsis* is generated through diacylglycerol kinase. Front Plant Sci **4**: 1

Browse J (2010) Saving the bilayer. Science **330**: 185–186

Chen M, Thelen JJ (2013) ACYL-LIPID DESATURASE2 is required for chilling and freezing tolerance in *Arabidopsis*. Plant Cell **25**: 1430–1444

Chen L, Liao B, Qi H, Xie LJ, Huang L, Tan WJ, Zhai N, Yuan LB, Zhou Y, Yu LJ, (2015a) Autophagy contributes to regulation of the hypoxia response during submergence in *Arabidopsis thaliana*. Autophagy **11**: 2233–2246

Chen QF, Xiao S, Chye ML (2008) Overexpression of the Arabidopsis 10-kilodalton acyl-coenzyme A-binding protein ACBP6 enhances freezing tolerance. Plant Physiol **148**: 304–315

Chen QF, Xu L, Tan WJ, Chen L, Qi H, Xie LJ, Chen MX, Liu BY, Yu LJ, Yao N, (2015b) Disruption of the *Arabidopsis* defense regulator genes *SAG101*, *EDS1*, and *PAD4* confers enhanced freezing tolerance. Mol Plant **8**: 1536–1549

Chinnusamy V, Ohta M, Kanrar S, Lee BH, Hong X, Agarwal M, Zhu JK (2003) ICE**1**: a regulator of cold-induced transcriptome and freezing tolerance in *Arabidopsis*. Genes Dev **17**: 1043–1054

Chinnusamy V, Zhu J, Zhu JK (2007) Cold stress regulation of gene expression in plants. Trends Plant Sci **12**: 444–451

Ding Y, Li H, Zhang X, Xie Q, Gong Z, Yang S (2015) OST1 kinase modulates freezing tolerance by enhancing ICE1 stability in *Arabidopsis*. Dev Cell **32**: 278–289

Fourrier N, Bédard J, Lopez-Juez E, Barbrook A, Bowyer J, Jarvis P, Warren G, Thorlby G (2008) A role for *SENSITIVE TO FREEZING2* in protecting chloroplasts against freeze-induced damage in *Arabidopsis*. Plant J **55**: 734–745

Foyer CH, Noctor G (2011) Ascorbate and glutathione: the heart of the redox hub. Plant Physiol **155**: 2–18

Fursova OV, Pogorelko GV, Tarasov VA (2009) Identification of ICE2, a gene involved in cold acclimation which determines freezing tolerance in *Arabidopsis thaliana*. Gene **429**: 98–103

Gómez-Merino FC, Brearley CA, Ornatowska M, Abdel-Haliem ME, Zanor MI, Mueller-Roeber B (2004) AtDGK2, a novel diacylglycerol kinase from *Arabidopsis thaliana*, phosphorylates 1-stearoyl-2-arachidonoyl-sn-glycerol and 1,2-dioleoyl-sn-glycerol and exhibits cold-inducible gene expression. J Biol Chem **279**: 8230–8241

Hernández ML, Whitehead L, He Z, Gazda V, Gilday A, Kozhevnikova E, Vaistij FE, Larson TR, Graham IA (2012) A cytosolic acyltransferase contributes to triacylglycerol synthesis in sucrose-rescued Arabidopsis seed oil catabolism mutants. Plant Physiol **160**: 215–225

Huang X, Li Y, Zhang X, Zuo J, Yang S (2010) The *Arabidopsis LSD1* gene plays an important role in the regulation of low temperature-dependent cell death. New Phytol **187**: 301–312

Iba K (2002) Acclimative response to temperature stress in higher plants: approaches of gene engineering for temperature tolerance. Annu Rev Plant Biol **53**: 225–245

Jammes F, Song C, Shin D, Munemasa S, Takeda K, Gu D, Cho D, Lee S, Giordo R, Sritubtim S, (2009) MAP kinases MPK9 and MPK12 are preferentially

expressed in guard cells and positively regulate ROS-mediated ABA signaling. Proc Natl Acad Sci USA **106**: 20520–20525

Katavic V, Reed DW, Taylor DC, Giblin EM, Barton DL, Zou J, Mackenzie SL, Covello PS, Kunst L (1995) Alteration of seed fatty acid composition by an ethyl methanesulfonate-induced mutation in *Arabidopsis thaliana* affecting diacylglycerol acyltransferase activity. Plant Physiol **108**: 399–409

Kaur G, Sharma A, Guruprasad K, Pati PK (2014) Versatile roles of plant NADPH oxidases and emerging concepts. Biotechnol Adv **32**: 551–563

Kilian J, Whitehead D, Horak J, Wanke D, Weinl S, Batistic O, D'Angelo C, Bornberg-Bauer E, Kudla J, Harter K (2007) The AtGenExpress global stress expression data set: protocols, evaluation and model data analysis of UV-B light, drought and cold stress responses. Plant J **50**: 347–363

Kim Y, Park S, Gilmour SJ, Thomashow MF (2013) Roles of CAMTA transcription factors and salicylic acid in configuring the low-temperature transcriptome and freezing tolerance of *Arabidopsis*. Plant J **75**: 364–376

Kuiper PJC (1970) Lipids in alfalfa leaves in relation to cold hardiness. Plant Physiol **45**: 684–686

Laloi C, Apel K, Danon A (2004) Reactive oxygen signalling: the latest news. Curr Opin Plant Biol **7**: 323–328

Li H, Ding Y, Shi Y, Zhang X, Zhang S, Gong Z, Yang S (2017) MPK3- and MPK6-mediated ICE1 phosphorylation negatively regulates ICE1 stability and freezing tolerance in *Arabidopsis*. Dev Cell **43**: 630–642.e4

Li W, Li M, Zhang W, Welti R, Wang X (2004) The plasma membrane-bound phospholipase Ddelta enhances freezing tolerance in *Arabidopsis thaliana*. Nat Biotechnol **22**: 427–433

Li W, Wang R, Li M, Li L, Wang C, Welti R, Wang X (2008) Differential degradation of extraplastidic and plastidic lipids during freezing and post-freezing recovery in *Arabidopsis thaliana*. J Biol Chem **283**: 461–468

Livak KJ, Schmittgen TD (2001) Analysis of relative gene expression data using real-time quantitative PCR and the 2(-Delta Delta C(T)) method. Methods **25**: 402–408

Miura K, Ohta M (2010) SIZ1, a small ubiquitin-related modifier ligase, controls cold signaling through regulation of salicylic acid accumulation. J Plant Physiol **167**: 555–560

Moellering ER, Benning C (2011) Galactoglycerolipid metabolism under stress: a time for remodeling. Trends Plant Sci **16**: 98–107

Moellering ER, Muthan B, Benning C (2010) Freezing tolerance in plants requires lipid remodeling at the outer chloroplast membrane. Science **330**: 226–228

Mueller SP, Unger M, Guender L, Fekete A, Mueller MJ (2017) Phospholipid:diacylglycerol acyltransferase-mediated triacylglyerol synthesis augments basal thermotolerance. Plant Physiol **175**: 486–497

Peters C, Kim SC, Devaiah S, Li M, Wang X (2014) Non-specific phospholipase C5 and diacylglycerol promote lateral root development under mild salt stress in *Arabidopsis*. Plant Cell Environ **37**: 2002–2013

Qi H, Xia FN, Xie LJ, Yu LJ, Chen QF, Zhuang XH, Wang Q, Li F, Jiang L, Xie Q, (2017) TRAF family proteins regulate autophagy dynamics by modulating AUTOPHAGY PROTEIN6 stability in *Arabidopsis*. Plant Cell **29**: 890–911

Qiu QS, Guo Y, Dietrich MA, Schumaker KS, Zhu JK (2002) Regulation of SOS1, a plasma membrane Na+/H+ exchanger in *Arabidopsis thaliana*, by SOS2 and SOS3. Proc Natl Acad Sci USA **99**: 8436–8441

Rajashekar CB, Zhou HE, Zhang Y, Li W, Wang X (2006) Suppression of phospholipase Dalpha1 induces freezing tolerance in Arabidopsis: response of cold-responsive genes and osmolyte accumulation. J Plant Physiol **163**: 916–926

Routaboul JM, Benning C, Bechtold N, Caboche M, Lepiniec L (1999) The *TAG1* locus of Arabidopsis encodes for a diacylglycerol acyltransferase. Plant Physiol Biochem **37**: 831–840

Saha S, Enugutti B, Rajakumari S, Rajasekharan R (2006) Cytosolic triacylglycerol biosynthetic pathway in oilseeds: molecular cloning and expression of peanut cytosolic diacylglycerol acyltransferase. Plant Physiol **141**: 1533–1543

Shockey JM, Gidda SK, Chapital DC, Kuan JC, Dhanoa PK, Bland JM, Rothstein SJ, Mullen RT, Dyer JM (2006) Tung tree DGAT1 and DGAT2 have nonredundant functions in triacylglycerol biosynthesis and are localized to different subdomains of the endoplasmic reticulum. Plant Cell **18**: 2294–2313

Steponkus PL (1984) The role of the plasma membrane in freezing injury and cold acclimation. Annu Rev Plant Physiol **35**: 543–584

Teige M, Scheikl E, Eulgem T, Dóczi R, Ichimura K, Shinozaki K, Dangl JL, Hirt H (2004) The MKK2 pathway mediates cold and salt stress signaling in *Arabidopsis*. Mol Cell **15**: 141–152

Thomashow MF (1999) Plant cold acclimation: freezing tolerance genes and regulatory mechanisms. Annu Rev Plant Physiol Plant Mol Biol **50**: 571–599

Thompson AR, Doelling JH, Suttangkakul A, Vierstra RD (2005) Autophagic nutrient recycling in *Arabidopsis* directed by the ATG8 and ATG12 conjugation pathways. Plant Physiol **138**: 2097–2110

Thorlby G, Fourrier N, Warren G (2004) The *SENSITIVE TO FREEZING2* gene, required for freezing tolerance in *Arabidopsis thaliana*, encodes a β-glucosidase. Plant Cell **16**: 2192–2203

Uemura M, Joseph RA, Steponkus PL (1995) Cold acclimation of *Arabidopsis thaliana* (effect on plasma membrane lipid composition and freeze-induced lesions). Plant Physiol **109**: 15–30

Verkleij AJ, De Maagd R, Leunissen-Bijvelt J, De Kruijff B (1982) Divalent cations and chlorpromazine can induce non-bilayer structures in phosphatidic acid-containing model membranes. Biochim Biophys Acta **684**: 255–262

Wang X (2004) Lipid signaling. Curr Opin Plant Biol **7**: 329–336

Welti R, Li W, Li M, Sang Y, Biesiada H, Zhou HE, Rajashekar CB, Williams TD, Wang X (2002) Profiling membrane lipids in plant stress responses: role of phospholipase D alpha in freezing-induced lipid changes in *Arabidopsis*. J Biol Chem **277**: 31994–32002

Xiao S, Chye ML (2011) Overexpression of *Arabidopsis ACBP3* enhances NPR1-dependent plant resistance to *Pseudomonas syringe* pv *tomato* DC3000. Plant Physiol **156**: 2069–2081

Xiao S, Gao W, Chen QF, Chan SW, Zheng SX, Ma J, Wang M, Welti R, Chye ML (2010) Overexpression of *Arabidopsis* acyl-CoA binding protein ACBP3 promotes starvation-induced and age-dependent leaf senescence. Plant Cell **22**: 1463–1482

Xing Y, Jia W, Zhang J (2008) AtMKK1 mediates ABA-induced CAT1 expression and H2O2 production via AtMPK6-coupled signaling in *Arabidopsis*. Plant J **54**: 440–451

Xu J, Carlsson AS, Francis T, Zhang M, Hoffman T, Giblin ME, Taylor DC (2012) Triacylglycerol synthesis by PDAT1 in the absence of DGAT1 activity is dependent on re-acylation of LPC by LPCAT2. BMC Plant Biol **12**: 4

Yamaguchi-Shinozaki K, Shinozaki K (2006) Transcriptional regulatory networks in cellular responses and tolerance to dehydration and cold stresses. Annu Rev Plant Biol **57**: 781–803

Yuan LB, Dai YS, Xie LJ, Yu LJ, Zhou Y, Lai YX, Yang YC, Xu L, Chen QF, Xiao S (2017) Jasmonate regulates plant responses to postsubmergence reoxygenation through transcriptional activation of antioxidant synthesis. Plant Physiol **173**: 1864–1880

Zhang M, Fan J, Taylor DC, Ohlrogge JB (2009a) DGAT1 and PDAT1 acyltransferases have overlapping functions in *Arabidopsis* triacylglycerol biosynthesis and are essential for normal pollen and seed development. Plant Cell **21**: 3885–3901

Zhang W, Wang C, Qin C, Wood T, Olafsdottir G, Welti R, Wang X (2003) The oleate-stimulated phospholipase D, PLDδ, and phosphatidic acid decrease H2O2-induced cell death in *Arabidopsis*. Plant Cell **15**: 2285–2295

Zhang Y, Zhu H, Zhang Q, Li M, Yan M, Wang R, Wang L, Welti R, Zhang W, Wang X (2009b) Phospholipase Dα1 and phosphatidic acid regulate NADPH oxidase activity and production of reactive oxygen species in ABA-mediated stomatal closure in *Arabidopsis*. Plant Cell **21**: 2357–2377

Zhao C, Wang P, Si T, Hsu CC, Wang L, Zayed O, Yu Z, Zhu Y, Dong J, Tao WA, (2017) MAP kinase cascades regulate the cold response by modulating ICE1 protein stability. Dev Cell **43**: 618–629.e5

Zou J, Wei Y, Jako C, Kumar A, Selvaraj G, Taylor DC (1999) The *Arabidopsis thaliana TAG1* mutant has a mutation in a diacylglycerol acyltransferase gene. Plant J **19**: 645–653